Unified Approach to Fast Convergent Row-Action-Type Iterative Methods for PET Image Reconstruction Using Multi Proximal Splitting

Kazuya Sadakata, Heejeong Kim, and Hiroyuki Kudo
University of Tsukuba, Tsukuba, Japan
Email: {s2230152, kudo}@cs.tsukuba.ac.jp

***Abstract*—Currently, Maximum Likelihood Expectation Maximization (MLEM) method and its accelerated version called Ordered-Subsets EM (OSEM) method have been used for image reconstruction in PET. It is known that the former has a drawback of slow convergence and the latter does not converge to a minimizer of cost function. Recently, image reconstruction methods using a new mathematical framework called proximal splitting have been actively studied. So far, most of the proximal splitting frameworks used for image reconstruction are based on splitting the cost function into two terms. With these conventional frameworks, it is impossible to obtain iterative methods that converge fast such as OSEM method and row-action-type iterative methods. To overcome this drawback, in this paper, we propose a unified approach to construct row-action-type iterative methods using three different types of multi proximal splitting frameworks. Results of simulation studies show that all the iterative methods obtained from the proposed approach can reduce the effect of statistical noise well and converge to a minimizer of the cost function with a high speed comparable to that of OSEM method.**

***Index Terms*—image reconstruction, PET, row-action-type acceleration**

I. Introduction

Currently, statistical iterative methods have been commonly used for image reconstruction in PET and SPECT [1]. In addition, statistical methods are also used in X-ray CT to improve image quality with low-dose measured data. It has been pointed out that analytical reconstruction methods may be completely replaced by the statistical iterative methods. The statistical methods are based on minimizing a cost function constructed from physical model of each imaging modality by using an iterative method. They have the three major advantages over the analytical methods. First, they can correct for image degradation due to various physical effects by incorporating them into the cost function. Second, they can reconstruct images with less noise. Third, they can be applied to cases where projection data is incomplete or where no analytical inversion formulae exist. Among the statistical methods, the most commonly used method is based on Maximum Likelihood (ML) estimation. Many of the statistical iterative reconstruction methods used in PET and SPECT are based on MLEM method proposed in 1982 [2]. The disadvantage of MLEM method is that it converges slowly leading to a requirement of a number of iterations to obtain a satisfactory image. To overcome this drawback, various speed-up methods have been studied.

One of the popular acceleration methods is the block iterative method, which divides the projection data into a number of subsets and each image update is performed by using only the subset sequentially according to some specified access order. This method was first proposed in 1994 and is called Ordered Subsets EM (OSEM) method [3]. In general, it is known that, by dividing the projection data into L subsets and using OSEM method, convergence can be accelerated by a factor of L. In addition, it is also known that the computational complexity of each iteration of OSEM method is almost the same as that of each iteration of MLEM method. However, OSEM method has a serious drawback that it does not converge to a minimizer of cost function when statistical noise is contained in the projection data.

Recently, image reconstruction using a new framework called proximal splitting has been studied for various reasons. For example, it allows to use non-differentiable regularization term such as Total Variation and it allows to derive a new class of statistical iterative reconstruction methods which have not been found in the existing literature. So far, the proximal splitting frameworks used for image reconstruction are still limited to the proximal splitting which splits a cost function into two terms. For example, these include Fast Iterative Shrinkage-Thresholding Algorithm (FISTA) [4], Alternating Direction Method of Multipliers (ADMM) [5], Chambolle-Pock algorithm [6], and so on. With these frameworks, it is difficult to derive iterative methods having the block-iterative or row-action structure like OSEM method that converge very quickly. To overcome this drawback, we propose a unified approach to derive row-action-type iterative methods using three different multi proximal splitting approaches, which are Passty's splitting, Dykstra-Boyle splitting, and Han's splitting. This framework allows us to derive statistical iterative methods which converge to a strict minimizer of cost function very fast. Finally, according to our best knowledge, the use of multi proximal splitting has not been studied in image reconstruction fields yet except for earlier work [7], [8].

Manuscript received October 28, 2021; revised April 2, 2022.

doi: 10.18178/joig.10.2.82-87

II. Methodology

A. Problem Definition

The objective of image reconstruction in PET is to reconstruct an image from measured projection data. The relation between the image and the projection data is expressed by:

$$\vec{\mathrm{b}} = \mathrm{Poisson}(A\vec{x}) \tag{1}$$

where $\vec{b} = (b_1, b_2, \dots, b_I)^T$ denotes the measured projection data, $\vec{x} = \left(x_1, x_2, \dots, x_J\right)^T$ denotes the image to be reconstructed, and $A = \{a_{ij}\}$ is the $I \times J$ system matrix.

B. Multi Proximal Splitting

First, we explain an important tool in this work called proximity operator. The definition of proximity operator is expressed as:

$$\mathrm{prox}_{\gamma f}(\vec{x}) = \mathrm{argmin}_{\vec{z}\in R^J}\left(f(\vec{z}) + \frac{1}{2\gamma}\|\vec{z} - \vec{x}\|^2\right) \tag{2}$$

where $\vec{z}, \vec{x} \in R^J$ and $\gamma > 0$ denotes the step-size parameter. We assume that $f(\vec{x})$ is a proper (non-necessarily differentiable) convex function. From equation (2), the proximity operator returns $\vec{z}$ minimizing the sum of a convex function $f(\vec{z})$ and the quadratic term $\|\vec{z} - \vec{x}\|^2/(2\gamma)$ for a given input $\vec{x}$. It is known that the proximity operator can be considered an extension of the classical gradient mapping $\nabla f(\vec{x})$, but it can be computed even in the case where $f(\vec{x})$ is non-differentiable. Next, we explain an alternative important concept called proximal splitting. Let us consider a convex minimization problem having the form expressed as:

$$\min_{\vec{x}\in R^J} f(\vec{x}) \equiv f_1(\vec{x}) + \cdots + f_n(\vec{x}) \tag{3}$$

where we assume that $f_1(\vec{x}), f_2(\vec{x}), \cdots, f_n(\vec{x})$ are (non-necessarily) convex functions. The proximal splitting is an efficient framework used to solve the minimization problem of Equation (3), when it is difficult to compute the direct proximity operator to the original cost function $f(\vec{x})$ but it is easy to compute the proximity operator corresponding to the split sub-cost functions $f_1(\vec{x}), f_2(\vec{x}), \cdots, f_n(\vec{x})$. Most of the proximal splitting frameworks used in image reconstruction so far have been based on the case where the number of split n is 2. However, by applying the frameworks proposed by Passty [9], Boyle and Dykstra [10], and Han [11] to PET image reconstruction, it becomes possible to derive a variety of fast convergent row-action-type iterative methods having the similar structure to that of OSEM method. Such research direction has not been investigated in image reconstruction fields yet. This paper demonstrates how to construct a new class of row-action type iterative methods using the multi-splitting and demonstrates that they work very well in practice.

We use three different frameworks of multi splitting to construct iterative formulae. Roughly, they have similar structures, but there is a small difference among the three. The first one called Passty's framework requires a step-size control which gradually diminishes the step-size $\gamma^{(k)}$ to zero as the iteration proceeds. This is a major drawback of Passty's framework. On the other hand, the second one called Boyle and Dykstra's framework does not require the step-size control, but it is necessary to add a perturbation term in the cost function, and the effect of perturbation term cannot be neglected in the solution. Finally, the third one called Han's framework does not have the above-mentioned disadvantages, *i.e.* the effect of perturbation term is diminished as the iteration proceeds without using the step-size control.

Hereafter, we assume that the cost function $f(\vec{x})$ used for image reconstruction is the negative log-likelihood in PET and the decomposition into the sub-cost function is performed as expressed as:

$$f(\vec{x}) = \sum_{i=1}^{I+1}[\overrightarrow{a_i^T}\vec{x} - b_i \log(\vec{a}_i^T\vec{x})]$$

$$f_i(\vec{x}) = \vec{a}_i^T\vec{x} - b_i \log(\vec{a}_i^T\vec{x}) \ \ (i = 1,2,\cdots,I)$$

$$f_{I+1}(\vec{x}) = \begin{cases} 0 \ \vec{x} \geq 0 \\ \infty \ \text{otherwise} \end{cases} \tag{4}$$

The iterative methods corresponding to each framework are summarized in Algorithm 1, 2, 3 without showing the detailed form of proximity operator $\mathrm{prox}(\cdot)$. The algorithms in a implementable form can be constructed by calculating the proximity operator $\mathrm{prox}_{\gamma f_i}(\vec{x})$ corresponding to each sub-cost function $f_i(\vec{x})$ for $i = 1,2,\dots,I$. Roughly, the processing procedure common to the three methods can be summarized as:

$$\begin{cases} \vec{x}^{(k,i+1)} = \mathrm{prox}_{\gamma^{(k)} f_i}\left(\vec{x}^{(k,i)}\right), \ \ (i = 1,2,\dots,I) \\ \vec{x}^{(k+1,1)} = \vec{x}^{(k,I+1)} \end{cases} \tag{5}$$

where k denotes the main iteration number and i denotes the sub-iteration number processing i-th sub-cost function. We also remark that each update indexed by (k,i) uses only single projection data b_i so that the algorithm structure. The image reconstruction methods having such structure is generally called row-action-type iterative algorithm, which converges very fast.

C. Deriving the Image Update Formula

Next, we show the procedure to derive the concrete image update equation. From the summary of Algorithms 1, 2, 3, to implement these methods, it is sufficient to calculate the detailed forms of proximity operators $\mathrm{prox}_{\gamma^{(k)} f_i(\vec{x})}(\cdot)(i = 1,2,\cdots,I)$ corresponding to the sub-cost functions $f_i(\vec{x})(i = 1,2,\cdots,I)$, which are common to Algorithms 1, 2, 3. Below, we describe the derivation only in the case of Passty's proximal splitting. We begin by representing the proximity operator corresponding to $f_i(x)$ as in Equation (6) and introducing the slack variable $z = \vec{a}_i^T\vec{x}$ to move the $\vec{a}_i^T\vec{x}$ part to outside of $f_i(\cdot)$ as a constraint. Then, we have:

$$\vec{x}^{(k,i+1)} = \mathrm{prox}_{\gamma^{(k)} f_i}\left(\vec{x}^{(k,i)}\right) =$$

$$\arg\min_{\vec{x}}\left(f_i(z) - b_i \log z + \frac{1}{2\gamma^{(k)}}\left\|\vec{x} - \vec{x}^{(k,i)}\right\|^2\right)$$

$$\text{subject to } z = \vec{a}_i^T\vec{x} \tag{6}$$

We can obtain the solution to the constrained minimization problem in Equation (6) by using the Lagrange function:

$$L(\vec{x}, z, \lambda) =$$

$$\frac{1}{2\gamma^{(k)}}\left\|\vec{x}-\vec{x}^{(k,i)}\right\|^2 + f_i(z) - b_i \log z + \lambda(z - \vec{a}_i^T\vec{x}) \quad (7)$$

where λ represents the Lagrange multiplier. By solving the equations obtained from $\frac{\partial L(\vec{x},z,\lambda)}{\partial \lambda} = 0, \frac{\partial L(\vec{x},z,\lambda)}{\partial z} = 0$, and $\frac{\partial L(\vec{x},z,\lambda)}{\partial \vec{x}} = 0$, we obtain the image update equation as:

$$x^{(k,i+1)} = x^{(k,i)} + \bar{t}a_i$$

$$\vec{x}^{(k,I+2)} = \left[\vec{x}^{(k,I+1)}\right]^+$$

$$\bar{t} = -\frac{\bar{p}-\sqrt{\bar{p}^2+\bar{q}}}{2\|a_i\|^2}, \bar{p} = a_i^T x^{(k,i)} + \gamma^{(k)}\|a_i\|^2$$

$$\bar{q} = 4\gamma^{(k)}\|a_i\|^2(b_i - a_i^T x^{(k,i)}) \quad (8)$$

Algorithm 1: Passty's Method

Input: Measured projection data $\vec{b}$, Initial image $\vec{x}^{(0)} = \vec{m}$
Output: Reconstructed image $\vec{x}^{(k)}$
Cost function: $\min_{\vec{x}} f(\vec{x}) \equiv \sum_{i=1}^{I} f_i(\vec{x})$

$k \leftarrow 0$

While iterating

$k \leftarrow k+1, \vec{x}^{(k,1)} = \vec{x}^{(k)}$

For all projection data$(i = 1,2,\cdots,I)$

$$\vec{x}^{(k,i+1)} = \text{prox}_{\gamma^{(k)} f_i(\vec{x})}\left(\vec{x}^{(k,i)}\right) \equiv$$

$$\min_{\vec{x}}\left(\frac{1}{2\gamma^{(k)}}\left\|\vec{x}-\vec{x}^{(k,i)}\right\|^2 + f_i(\vec{x})\right)$$

$$\vec{x}^{(k+1)} = \vec{x}^{(k,I+1)}$$

$\gamma^{(k)} \to 0 (k \to \infty)$

Algorithm 2: Boyle and Dykstra's Method

Input: Measured projection data $\vec{b}$, Initial image $\vec{x}^{(0)} = \vec{m}$
Output: Reconstructed image $\vec{x}^{(k)}$
Cost function: $\min_{\vec{x}} f(\vec{x}) \equiv \frac{1}{2\gamma}\|\vec{x}-\vec{m}\|^2 + \sum_{i=1}^{I} f_i(\vec{x})$

$k \leftarrow 0, \vec{y}_i^{(0)} = 0 (i = 1,2,\ldots,I)$

While iterating

$k \leftarrow k+1$

$\vec{x}^{(k,1)} = \vec{x}^{(k)}$

For all projection data $i = 1,2,\cdots,I$

$$\vec{x}^{(k,i+1)} = \text{prox}_{\gamma f_i(\vec{x})}\left(\vec{x}^{(k,i)} + \vec{y}_i^{(k)}\right) \equiv$$

$$\min_{\vec{x}}\left(\frac{1}{2\gamma}\left\|\vec{x}-(\vec{x}^{(k,i)} + \vec{y}_i^{(k)})\right\|^2 + f_i(\vec{x})\right)$$

$$\vec{y}_i^{(k+1)} = \vec{y}_i^{(k)} + \vec{x}^{(k,i)} - \vec{x}^{(k,i+1)}$$

End for

$\vec{x}^{(k+1)} = \vec{x}^{(k,I+1)}$

End while

$\gamma > 0$

Algorithm 3: Han's Method

Input: Measured projection data $\vec{b}$, Initial image $\vec{x}^{(0)} = \vec{m}$
Output: Reconstructed image $\vec{x}^{(k)}$
Cost function: $\min_{\vec{x}} f(\vec{x}) \equiv \sum_{i=1}^{I} f_i(\vec{x})$

$k \leftarrow 0, \vec{y}_i^{(0)} = 0 (i = 1,2,\ldots,I), \vec{z}^{(0)} = 0$

While iterating

$k \leftarrow k+1$

$\vec{x}^{(k,1)} = \vec{x}^{(k)} + \vec{z}^{(k)}$

For all projection data $i = 1,2,\cdots,I$

$$\vec{x}^{(k,i+1)} = \text{prox}_{\gamma f_i(\vec{x})}\left(\vec{x}^{(k,i)} + \vec{y}_i^{(k)}\right) \equiv$$

$$\min_{\vec{x}}\left(\frac{1}{2\gamma}\left\|\vec{x}-(\vec{x}^{(k,i)} + \vec{y}_i^{(k)})\right\|^2 + f_i(\vec{x})\right)$$

$$\vec{y}_i^{(k+1)} = \vec{y}_i^{(k)} + \vec{x}^{(k,i)} - \vec{x}^{(k,i+1)}$$

End for

$\vec{x}^{(k+1)} = \vec{x}^{(k,I+1)}$

$\vec{z}^{(k+1)} = \vec{z}^{(k)} + \vec{x}^{(k,I+1)} - \vec{x}^{(k,1)}$

End while

$\gamma > 0$

The final row-action-type PET image reconstruction method using Passty's multi proximal splitting is summarized in Algorithm 4. Finally, we mention that the iterative methods corresponding to Boyle and Dykstra's splitting and Han's splitting can be obtained by following the same calculation steps as above. We omit the final algorithm summary to save the space.

Algorithm 4: Row-action-type accelerated PET image reconstruction algorithm using Passty's method

Input: Measured projection data $\vec{b}$ as an I-dimensional vector, Initial image $\vec{x}^{(0)}$ as an N × N-dimensional vector, step-size control parameters $(\gamma^{(0)}, \epsilon)$
Output: Reconstructed image $\vec{x}^{(k)}$ as an N × N -dimensional vector.

$k \leftarrow 0$

While iterating

$\gamma^{(k)} = \frac{\gamma^{(0)}}{1+\epsilon k}, \vec{x}^{(k,i)} = \vec{x}^{(k)}$

For all projection data$(i = 1,2,\cdots,I)$

$$\bar{p} = \vec{a}_i^T\vec{x}^{(k,i)} + \gamma^{(k)}\|\vec{a}_i\|^2,$$

$$\bar{q} = 4\gamma^{(k)}\|\vec{a}_i\|^2(b_i - \vec{a}_i^T\vec{x}^{(k,i)})$$

$$\bar{t} = -\frac{\bar{p}-\sqrt{\bar{p}^2+\bar{q}}}{2\|\vec{a}_i\|^2}$$

$$\vec{x}^{(k,i+1)} = \vec{x}^{(k,i)} + \bar{t}\vec{a}_i$$

End for

$\vec{x}^{(k,I+2)} = \left[\vec{x}^{(k,I+1)}\right]^+$

$\vec{x}^{(k+1)} = \vec{x}^{(k,I+2)}$

$k \leftarrow k+1$

End while

$\gamma^{(k)} \to 0 (k \to \infty)$

III. Experimental Results

A. Numerical Simulation

We compared the four iterative reconstruction methods, *i.e.* OSEM method, Passty's method (Proposed Method 1), Boyle and Dykstra's method (Proposed Method 2), and Han's method (Proposed Method 3) using Shepp-Logan numerical phantom. The phantom image consisted of 256×256 (pixels) and the projection data were computed by the parallel-beam geometry with 256 (bins) and 256 (views) over the $180°$ angular range. The statistical noise corresponding to the number of total photon counts 5×10^5 was added to the projection data. In implementing the proposed three methods, the value of step size γ was set to 15, and the initial image in the iteration was set to an image having uniform intensity within the inscribed circle to the image matrix. The definition of used PET phantom was same as that described in Vardi [12]. With respect to the regularization, *i.e.* smoothing, we applied a post-smoothing with a Gaussian filter having pre-defined a FWHM value after the iteration was stopped, which is the standard regularization method used in clinical PET scanners. The size of Gaussian kernel was 3×3 (pixels) and the value of FWHM was 2.35. The phantom consisted of eight ellipses and was chosen as a simplified imitation of brain's metabolic activity, where the skull metabolizes at a low rate of 0.1 and the ventricles, tumors, and so on, metabolize at rates between 0.3 and 2.0. Reconstructed images are shown in Fig. 1. It is observed that the image by OSEM method suffers from non-acceptable amplification of statistical noise, mainly because it does not converge to a minimizer of cost function. It is well-known that the noise property of OSEM method is much worse compared to the exactly convergent method such as MLEM method. However, the three proposed methods succeed in significantly reducing the effect of noise leading to nicer images. Next, to evaluate the results quantitatively, Table I shows the average values of Structural Similarity (SSIM) and Peak Signal-to-Noise Ratio (PSNR) after 100 image reconstructions when the number of iterations is 5. In addition, Table I shows the average computation times per iteration.

B. Application to Real Data of Whole-Body PET

We used 3D PET real data corresponding to whole-body FDG scan to evaluate the four methods. The reconstructed image size was $128 \times 128 \times 278$ (voxels), and the projection data consisted of 128 (bins) × 128 (views) × 278 (slices). In implementing the three proposed methods, the value of step size γ was set to 300. Similarly to the case of numerical phantom, OSEM method, Proposed Method 1, Proposed Method 2, Proposed Method 3 were compared. We show vertical slices of the reconstructed images in Fig. 2, which demonstrates that the noise performances of the proposed three methods are much better compared to OSEM method as in the case of numerical simulations. Furthermore, the speed of convergence were comparable in all the implemented methods because all the methods have a row-action structure.

TABLE I. Average Values of SSIM and PSNR and Computation Time with Statistical Noise

	SSIM	PSNR [dB]	Average Time [sec]
OSEM method	0.5316	17.15	6.817
Proposed method1	0.6458	25.69	8.329
Proposed method 2	0.6698	26.17	8.369
Proposed method 3	0.6695	26.16	8.385

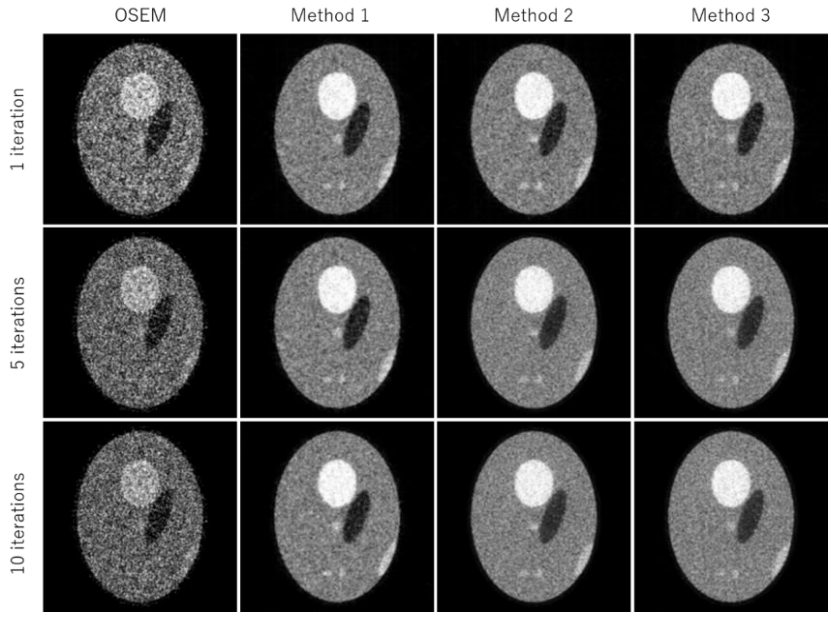

Figure 1. Reconstructed images by OSEM method, Method1 (Passty's), Method2 (Boyle and Dykstra's), and Method3 (Han's).

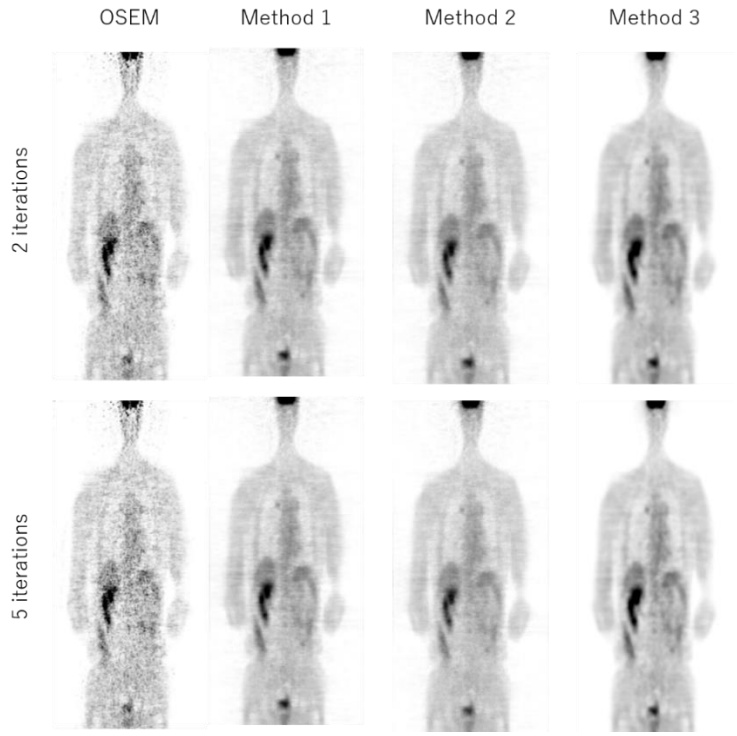

Figure 2. Reconstructed image of 3D whole-body real data by OSEM method, Method1, Method2, and Method3.

IV. Conclusion

In this paper, we proposed a unified approach to derive a class of row-action-type PET iterative reconstruction methods using multi proximal splitting, which have not been used in tomographic image reconstruction fields yet. The simulation results as well as the real data experiments demonstrate that all the methods are able to produce better images than standard OSEM method with a comparable convergence speed. In this work, we derived iterative methods for PET image reconstruction, but we are planning to extend the proposed methods to other imaging modalities such as X-ray CT in future work. Furthermore, in the simulation study reported in this paper, we considered only a single case of total photon count and a single empirically determined step-size parameter. We need to perform further experiments to understand what kind of changes occur in the performances when these parameters are changed.

Conflict of Interest

The authors declare no conflict of interest.

Author Contributions

All the authors contributed to the algorithm developments. Kazuya Sadakata and Heejeong Kim performed the implementation studies. Kazuya Sadakata and Hiroyuki Kudo wrote the paper. All the authors approved the final version.

References

[1] *Medical Imaging Handbook (in Japanese)*, The Japanese Society of Medical Imaging Technology, 2012, pp. 55-67.

[2] L. A. Shepp and Y. Vardi, "Maximum likelihood reconstruction for emission tomography," *IEEE Trans. Med. Imaging*, vol. 1, pp. 113-122, 1982.

[3] H. M. Hudson and R. S. Larkin, "Accelerated image reconstruction using ordered subsets of projection data," *IEEE Trans. Med. Imaging*, vol. 13, pp. 601-609, 1994.

[4] A. Beck and M. Teboulle, "A fast iterative shrinkage-thresholding algorithm for linear inverse problems," *SIAM J. Imaging Sciences*, vol. 2, no. 1, pp. 183-202, 2009.

[5] S. Boyd, N. Parikh, E. Chu, B. Peleato, and J. Eckstein, "Distributed optimization and statistical learning via the alternating direction method of multipliers," *FTML*, vol. 3, no. 1, pp. 1-122, 2010.

[6] A. Chambolle and T. Pock, "A first-order primal-dual algorithm for convex problems with applications to imaging," *J. Mathmetical Imaging and Vision*, vol. 40, pp. 120-145, 2011.

[7] J. Dong and H. Kudo, "Accelerated algorithm for compressed sensing using nonlinear sparsifying transform in CT image reconstruction," *Medical Imaging Technology*, vol. 35, no. 1, pp. 63-73, 2017.

[8] S. Rose, M. S. Andersen, E. Y. Sidky, and X. Pan, "Noise properties of CT images reconstructed by use of constrained total-variation, data-discrepancy minimization," *Medical Physics*, vol. 42, no. 5, pp. 2690-2698, 2015.

[9] G. B. Passty, "Ergodic convergence to a zero of the sum of monotone operators in Hilbert space," *J. Math. Anal. Appl.*, vol. 72, pp. 383-390, 1979.

[10] J. P. Boyle and R. L. Dykstra, "A method for finding projections onto the intersection of convex sets in Hilbert spaces," *Lecture Notes in Statistics*, vol. 37, pp. 28-47, 1986.

[11] S. P. Han, "A decomposition method and its application to convex programming," *Math. Oper. Res.*, vol. 14, pp. 237-248, 1989.

[12] Y. Vardi, L. A. Shepp, and L. Kaufman, "A statistical model for positron emission tomography," *Journal of the American Statistical Association*, vol. 80, no. 389, pp. 8-20, 1985.

Kazuya Sadakata received the B.E. degree from the Division of Information and Electronic System Engineering, NIT Sendai college, Japan, in 2020. He is a student in the Degree Programs in Systems and Information Engineering Graduate school of Science and Technology, University of Tsukuba, Japan. His major research field is PET image reconstruction.

Heejeong Kim received the B.E. degree from the Department of Advanced Robotics, Chiba Institute of Technology, Japan, in 2020. She is a student in the Degree Programs in Systems and Information Engineering Graduate school of Science and Technology, University of Tsukuba, Japan. Her major research field is CT image reconstruction.

Hiroyuki Kudo received the B.Sc. degree from the Department of Electrical Communications, Tohoku University, Japan, in 1985, and the Ph.D. degree from the Graduate School of Engineering, Tohoku University, in 1990. In 1992, he joined the University of Tsukuba, Japan. He is currently a Professor with the Division of Information Engineering, Faculty of Engineering, Information and Systems, University of Tsukuba, Japan. His research areas include medical imaging, image processing, and inverse problems. In particular, he is actively working on tomographic image reconstruction for X-ray CT, PET, SPECT, and electron tomography. He received best paper awards more than 10 times from various international and Japanese societies. He received the IEICE (The Institute of Electronics, Information, and Communication Engineers, Japan) Fellow award for his contributions on "cross-sectional image reconstruction methods in medical computed tomography". In 2018, he obtained Commendation for Science and Technology by the Minister of Education, Culture, Sports, Science and Technology for his contributions on "research on design method and image reconstruction method for new CT". For 2011-2016, he was an Editor-in-Chief of the Journal of Medical Imaging Technology (MIT). From 2020, he is a president of Japanese Society of Medical Imaging Technology (JAMIT).